



## COMPARATIVE ANALYSIS OF EAST-WEST AND SOUTH-NORTH SINGLE-AXIS SOLAR TRACKING SYSTEMS

\* Kutbay SEZEN 

*Alanya Alaaddin Keykubat University, ALTSO Vocational School of Higher Education, Antalya TÜRKİYE*  
[kutbay.sezen@alanya.edu.tr](mailto:kutbay.sezen@alanya.edu.tr)

### *Highlights*

- Solar radiation gain
- Single-axis tracking
- East-west orientation
- South-north orientation
- Konya region tracking angles



## COMPARATIVE ANALYSIS OF EAST-WEST AND SOUTH-NORTH SINGLE-AXIS SOLAR TRACKING SYSTEMS

\* Kutbay SEZEN 

*Alanya Alaaddin Keykubat University, ALTSO Vocational School of Higher Education, Antalya TÜRKİYE*  
[kutbay.sezen@alanya.edu.tr](mailto:kutbay.sezen@alanya.edu.tr)

(Received: 14.11.2024; Accepted in Revised Form: 24.05.2025)

**ABSTRACT:** As global energy demand continues to grow, maximizing the efficiency of solar energy as a renewable resource is increasingly critical. Solar tracking systems offer an effective solution by optimizing panel orientation to capture more solar radiation. This study evaluates the annual and seasonal solar radiation gains of single-axis tracking systems, comparing east-west and south-north orientations with fixed-tilt and horizontal surfaces. Daily, monthly, and annual radiation values were calculated based on the average day of each month, and hourly radiation variations were analyzed for June and December. Annually, the east-west tracking system increased radiation capture by approximately 30% compared to a horizontal surface and 19% compared to a fixed-tilt surface, while the south-north system achieved gains of 16% and 6%, respectively. In June, the east-west system outperformed the south-north setup by 2.02 kWh/m<sup>2</sup> daily (a 29% increase), whereas in December, the south-north system collected 0.43 kWh/m<sup>2</sup> more per day (a 25% increase) due to better alignment with the sun's lower southern path. The method used in this study is based on manual, equation-driven modeling, aiming to enhance transparency and provide a cost-effective, software-independent tool. The calculated hourly tracking angles can be applied to future systems in the same region, while the overall procedure can be easily adapted to other locations by incorporating region-specific input parameters.

**Keywords:** *Solar Radiation Gain, Single-Axis Tracking, East-West Orientation, South-North Orientation, Konya Region Tracking Angles*

### 1. INTRODUCTION

The global demand for energy continues to rise sharply due to rapid industrialization, urban expansion, and population growth. Traditionally, fossil fuels have dominated the global energy mix, but their environmental consequences—including greenhouse gas emissions and air pollution—have intensified the need for sustainable alternatives. Among renewable energy sources, solar energy is particularly attractive due to its abundance, accessibility, and environmental friendliness.

Solar energy can be harnessed through various technologies, the most common of which are photovoltaic (PV) systems. PV systems are widely adopted due to their modularity, scalability, and relatively low maintenance requirements. Improving the efficiency of photovoltaic (PV) systems has become a key research area in the transition to clean energy [1].

Enhancing the power output of photovoltaic (PV) systems remains a central focus in renewable energy research, with numerous strategies proposed to improve efficiency. One widely studied approach involves concentrated photovoltaic systems (CPVS), which utilize reflective mirrors to direct and intensify solar radiation onto a smaller PV surface. In this context, low-concentration PV systems (LCPVS) have gained attention due to their simplicity and cost-effectiveness. Studies by Kolaroudi et al. [2, 3] showed that LCPVS using mirrors combined with water-based cooling systems can increase power output by up to three times compared to standard flat-panel systems, while also reducing the required PV surface area. Additionally, their review study [4] provided a comprehensive comparison of LCPVS with other systems, emphasizing the benefits of using mirrors and passive cooling to improve system efficiency and reduce installation costs.

In parallel, cooling techniques have been extensively investigated to mitigate thermal losses in PV

\*Corresponding Author: Kutbay SEZEN, [kutbay.sezen@alanya.edu.tr](mailto:kutbay.sezen@alanya.edu.tr)

panels. A recent review by Utomo et al. [5] classified cooling strategies into conductive, convective, and radiative methods, highlighting the effectiveness of nanofluids and phase change materials (PCMs) in reducing panel temperatures by up to 40°C and enhancing energy output by approximately 1.67%.

Beyond system design, material innovations also play a crucial role in efficiency improvement. Emerging photovoltaic technologies such as organic, dye-sensitized, perovskite, and quantum dot solar cells offer advantages like lightweight construction and lower production costs. However, as noted by Gressler et al. [6], these advanced systems require careful life cycle assessment due to environmental and material sustainability concerns. In addition to material advances, bifacial PV panels have demonstrated performance gains by harvesting both direct sunlight and reflected radiation from the ground. According to Aksoy and Çalık [7], bifacial systems installed over white or sandy surfaces generated up to 6.4% more energy annually than monofacial panels under identical conditions, proving especially effective in high-reflectance environments.

Cleaning systems have also shown measurable effects on efficiency. Park et al. [8] developed a low-cost robotic cleaning solution that increased panel voltage and current by 8.02% and 18.78%, respectively, emphasizing the role of maintenance in long-term performance. Optimal panel tilt is another factor influencing solar gains. Kabul et al. [9] analyzed exergy potential across varying tilt angles in Turkey and found that a 30° tilt yielded the best year-round efficiency, which aligns with typical design practices for fixed and tracking systems.

One of the most effective strategies for improving PV system performance is solar tracking, which enhances energy harvest by adjusting panel orientation to follow the sun's movement. Solar tracking systems can be either single-axis or dual-axis. Single-axis systems have a simpler structure, allowing panels to move along only one axis. These systems track the sun's daily movement in either the east-west or south-north direction to enhance energy gains. Dual-axis systems, on the other hand, can track both the azimuth and elevation angles of the sun, enabling them to collect more solar radiation than single-axis systems. Although dual-axis systems come with higher costs and complexity, they offer a greater capacity for solar energy collection.

Experimental studies have consistently demonstrated that tracking systems outperform fixed configurations. Akpınar et al. [10] observed that solar tracking improved energy output of thermal and photovoltaic panels by up to 75.2% and 26.3%, respectively, depending on panel type. Similarly, Singh et al. [11] and Kabilan et al. [12] developed low-cost automatic tracking systems using LDRs and microcontrollers, both reporting significant improvements in current, voltage, and power output over fixed setups.

Review studies that provide a comprehensive examination of the technical and economic aspects of solar tracking systems, along with tracking control methods in light of current researches, offer valuable insights on the subject. Kumba et al. [13] compiled studies on solar tracking systems, evaluating the performance and energy efficiency of passive, active, single-axis, dual-axis, and hybrid systems under various environmental conditions. This study summarizes the energy production increases achieved by different tracking systems and highlights potential areas for future technological advancement. Kazem et al. [14] gathered studies focusing on the design, cost, and efficiency of solar tracking systems, providing critical information on how advanced technologies—particularly artificial intelligence and machine learning—can be used to optimize these systems. Kuttybay et al. [15] assessed studies examining the geographic, climatic, and design factors affecting the efficiency of solar tracking systems, summarizing the efficiency gains of single and dual-axis systems compared to fixed systems. Bahrami et al. [16] conducted a technical and economic comparison of fixed, single-axis, and dual-axis tracking systems in Nigeria, highlighting variations in annual energy yield and levelized cost of electricity. Their results offer practical guidelines for selecting the most cost-effective tracking options in diverse geographical contexts. Together, these studies offer a holistic perspective on the technical and economic parameters that should be considered in the development and implementation of solar tracking systems.

In the literature, studies on solar tracking systems often focus on either the control methods used to operate these systems or the radiation gains achieved by tracking surfaces compared to fixed or

horizontal surfaces in specific regions. This study, however, examines radiation gains based on the hourly maximum power angle, analyzing both east-west and south-north tracking directions rather than the specific control elements managing the tracking system. As a result, solar radiation gains provided by one axis tracking systems in different orientations are explored in detail on an annual, monthly, and hourly basis.

Some studies focused on solar tracking control methods include the following. Kumba et al. [17] proposed a novel single-axis solar tracking system based on the second-class lever principle, eliminating the need for an external motor by balancing the PV panel's mass with that of water and analyzing the resulting power output increase compared to traditional systems. Alshaabani [18] developed a low-cost, real-time single-axis solar tracking system that monitors the sun's angle using four photodiodes. Er and Balcı [19] designed a dual-axis solar tracking system without using any sensors, programming it via a PLC to move based on the sun's angle and observing an increase in efficiency. Toylan [20] designed a dual-axis solar tracking system using a fuzzy logic controller optimized by a genetic algorithm, reporting that this system outperformed fixed PV panels. Attou et al. [21] proposed a control system aimed at enhancing energy efficiency in PV systems through maximum power point tracking (MPPT) using the Perturb & Observe algorithm. Khan and Tacer [22] developed an MPPT controller based on a microinverter, improving PV system performance in terms of dynamic response and efficiency. Arpacı et al. [23] compared a fuzzy logic controller and the Perturb & Observe algorithm for MPPT, analyzing their effectiveness in tracking the maximum power point in PV systems. Baçoğlu et al. [24] developed an Arduino-based dual-axis solar tracking system for a 45W PV panel, achieving higher efficiency than static PV systems. Alhaj Omar et al. [25] conducted a comparative analysis of three commonly used MPPT algorithms—Perturb & Observe, Incremental Conductance, and Fuzzy Logic—under varying weather conditions, finding that the Fuzzy Logic algorithm showed best performance with its fast response.

Dual-axis tracking systems have been extensively researched due to their ability to offer the highest efficiency in solar energy harvest. Sungur [26] reported that a dual-axis solar tracking system controlled by a PLC in Turkey produced 42.6% more energy compared to a fixed system. Yılmaz et al. (2015) indicated that a dual-axis tracking system used in a 4.6 kW PV system achieved a 34% increase in energy harvest over a fixed system. Üçgül and Şenol (2016) observed that microcontroller-controlled dual-axis systems yielded 28% more power daily than fixed panels. Şenol et al. (2021) reported a 9% efficiency gain with their dual-axis solar tracking system, which employed a fuzzy logic control algorithm. Garip (2021) demonstrated that dual-axis systems provided 25–35% higher energy harvest compared to static systems, while Bilhan and Etcı (2021) found that dual-axis systems in the Konya region produced 16.7% more energy than fixed systems.

However, some studies have noted that the benefits of tracking systems may be limited in certain conditions. Kelly and Gibson [27] developed an algorithm that captured 50% more energy in a horizontal position compared to dual-axis tracking on cloudy days. Quesada et al. [28] showed that, particularly at higher latitudes, a horizontal position captured more radiation than a fixed angle on cloudy days, suggesting that solar tracking strategies should be optimized for such conditions.

Single-axis solar tracking systems are widely studied due to their ability to increase efficiency with lower costs and less complexity compared to dual-axis tracking. Öztürk et al. [29] reported that a single-axis solar tracking system with bifacial PV modules in Konya achieved 75.5% energy efficiency and a maximum electrical efficiency of 36.42%, with a sustainability index of 1.29. Kayrı [30] developed a single-axis solar tracking system designed to improve the long-term durability of modules against atmospheric conditions, demonstrating a 30.84% increase in efficiency on an annual basis. Arslanoğlu and Yiğit [31] highlighted that placing parabolic trough-type single-axis solar collectors in a south-north orientation can enhance thermal energy production efficiency, making this system ideal for high-temperature energy generation. Alomar et al. [32] compared the performance of fixed, single-axis, and dual-axis systems, noting that single-axis systems produced 16.5% more electricity than fixed systems and reduced CO<sub>2</sub> emissions by approximately 4,000 tons annually. Azam et al. [33] examined a single-

axis system that employed an intermittent tracking algorithm rather than continuous tracking, finding that it provided 1.12% less radiation gain than a fixed system but reduced its own energy consumption by 34%. Celen et al. [34] conducted an energy and exergy analysis of solar collectors at varying tilt angles in Erzincan, finding that optimal tilt angles significantly impact radiation capture and efficiencies, with maximum energy and exergy efficiencies of 74.2% and 9.7%, respectively.

Distinctively in this study, a single-axis tracking system is analyzed in both east-west and south-north orientations, comparing these two configurations to fixed-angle and horizontal surfaces within the Konya province of Turkey. The selected region was chosen based on its high solar energy potential and favorable geographical characteristics, as highlighted by Doğan and Karakılıç [35]. Unlike many existing works that emphasize control mechanisms or sensor systems, this study focuses on the radiation gains achieved by each orientation on annual, monthly, and hourly scales. The analysis was conducted using the monthly average day method, with daily tracking divided into hourly intervals to establish a more holistic and simplified modeling framework. Inspired by the emphasis on simple and easy-to-maintain tracking designs discussed by Kuttybay et al. [15], this study proposes a semi-tracking approach that reduces system complexity and energy consumption while maintaining significant radiation gains.

The instantaneous and daily radiation values on inclined surfaces were calculated based on published theoretical and empirical formulas. Mathematical models for east-west tracking, south-north tracking, fixed-tilt, and horizontal surfaces were developed in MS-Excel. Using the iterative solution provided by the Solver add-in, the optimal angle values that yield the highest hourly radiation gain were determined for each month's average day for the study location. The annual total solar radiation gain of the four surfaces was compared, and the monthly average daily radiation values were calculated. Additionally, the hourly instantaneous radiation values for June and December, representing the summer and winter solstices, were compared. The resulting hourly tracking angle change table for each month's average day in Konya provides valuable data for future single-axis solar tracking systems in the region. Furthermore, the calculation method presented in this study can be easily adapted to other geographical locations worldwide to generate site-specific angle tables for optimized tracking performance.

In the literature, studies on solar tracking systems often emphasize either the control methods used to operate these systems or the radiation gains achieved by tracking surfaces relative to fixed or horizontal configurations in specific regions. This study, however, focuses on radiation gains calculated based on the hourly maximum power angle, analyzing both east-west and south-north tracking directions independently of the specific control mechanisms. Accordingly, the radiation gains of one-axis tracking systems in different orientations are explored in detail on an annual, monthly, and hourly basis.

While many commercial solar simulators can produce comparable results using built-in empirical models, this study deliberately employs a manual, equation-based approach to promote transparency and scientific clarity. By explicitly applying and visualizing the underlying solar geometry and radiation equations, the method offers deeper insight into the core principles driving solar tracking performance. Moreover, this approach is cost-effective, independent of proprietary software, and easily adaptable to other locations through region-specific input adjustments or empirical model selection.

## 2. MATERIAL AND METHODS

In this study, solar radiation gains were compared across four configurations: a single-axis tracking system oriented east-west, a single-axis tracking system oriented south-north, a south-facing surface with an annual fixed optimal tilt angle, and a horizontal surface. First, the theoretical calculation method for daily solar radiation on inclined and horizontal surfaces is explained, followed by a detailed calculation of instantaneous solar radiation on an inclined surface to guide the calculation of daily solar radiation for the single-axis tracking system. The mathematical models developed by Liu and Jordan [36, 37] and the empirical equations compiled by Yiğit and Atmaca [38] were used in the calculations.

## 2.1. Calculation of Total Daily Solar Radiation on Horizontal and Inclined Surfaces

The total solar radiation falling on a horizontal surface,  $H$ , can be determined using Equation 1:

$$H = K_T \cdot H_o \quad (1)$$

Where  $K_T$  is the clearness index, and  $H_o$  represents the total solar radiation falling on a horizontal surface outside the atmosphere, calculated with Equation 2:

$$H_o = \frac{24 \times 3600 G_{sc}}{\pi} \left[ 1 + 0.033 \cos\left(\frac{360d}{365}\right) \right] \cdot \left[ \cos\phi \cos\delta \sin\omega_s + \frac{2\pi\omega_s}{360} \sin\phi \sin\delta \right] \quad (2)$$

Here,  $\phi$  is the latitude angle,  $d$  is the day of the year,  $\delta$  is the declination angle, and  $\omega_s$  is the sunset hour angle. The solar constant  $G_{sc}$  is the solar radiation intensity falling on the horizontal plane outside the atmosphere and can be taken as  $1367 \text{ W/m}^2$ .

The declination angle  $\delta$ , which is the angle between the sun's rays and the equatorial plane, is calculated based on the day of the year  $d$  using Equation 3:

$$\delta = 23,45 \sin\left(360 \frac{284+d}{365}\right) \quad (3)$$

For monthly average daily total solar radiation calculations, the average day value ( $d$ ) for each month, as listed in Table 1, can be used.

**Table 1.** Average day value ( $d$ ) of each month [38]

Month	Jan	Feb	Mar	Apr	May	Jun	Jul	Aug	Sep	Oct	Nov	Dec
Avg. Day	17	47	75	105	135	162	198	228	258	288	318	344

The sunset hour angle  $\omega_s$  is defined by Equation 4:

$$\omega_s = \cos^{-1}(-\tan\phi \tan\delta) \quad (4)$$

After calculating the solar radiation on a horizontal surface  $H_o$ , the clearness index  $K_T$ , given by Equation 5, can be used to find the total daily solar radiation on an inclined surface:

$$K_T = \left( a + b \frac{n}{N} \right) \quad (5)$$

Where  $N$  is the day length,  $n$  is the actual sunshine duration, and  $a$  and  $b$  are regional constants defined by Equation 6 and Equation 7, respectively:

$$a = 0,103 + 0,000017Z + 0,198 \cos(\phi - \delta) \quad (6)$$

$$b = 0,533 - 0,165 \cos(\phi - \delta) \quad (7)$$

Here,  $Z$  represents the altitude (in meters). The day length  $N$  can be calculated using Equation 8:

$$N = \frac{2}{15} \omega_s \quad (8)$$

The actual sunshine duration ( $n$ ) for a given region is based on observational data and, for Turkish provinces, is published by Güneş Enerji Potansiyeli Atlası (GEPA) [39]. Table 2 provides the average monthly sunshine duration for studied province.

**Table 2.** Monthly sunshine duration ( $n$ ) for Konya (hour) [39]

Month	Jan	Feb	Mar	Apr	May	Jun	Jul	Aug	Sep	Oct	Nov	Dec
Konya	4,19	5,51	6,88	8,03	9,46	11,28	11,97	11,36	9,79	7,35	5,53	3,93

The total daily solar radiation on a horizontal surface,  $H$ , consists of direct  $H_b$  and diffuse  $H_d$  components:

$$H = H_d + H_b \quad (9)$$

The relationship between diffuse radiation  $H_d$  and total radiation  $H$  is defined by Equation 10:

$$H_d = H(1 - 1,13K_T) \quad (10)$$

The total daily solar radiation  $H_T$  on an inclined surface can be calculated using Equation 11:

$$H_T = H_b \bar{R}_b + H_d \left( \frac{1 + \cos\beta}{2} \right) + H \rho \left( \frac{1 - \cos\beta}{2} \right) \quad (11)$$

Where  $\beta$  is the tilt angle of the surface, and  $\rho$  is the reflection coefficient, which can be taken as 0.7 on snowy days and 0.2 on other days [38]. For Konya, December, January, and February are typically snowy months, according to Meteoroloji Genel Müdürlüğü (MGM) data [40].

The ratio of daily direct radiation on an inclined surface to daily direct radiation on a horizontal surface  $\bar{R}_b$  is defined by Equation 12:

$$\bar{R}_b = \frac{\cos(\phi - \beta) \cos\delta \sin\omega_s' + (\pi/180) \omega_s' \sin(\phi - \beta) \sin\delta}{\cos\phi \cos\delta \cos\omega_s + (\pi/180) \omega_s \sin\phi \sin\delta} \quad (12)$$

Here,  $\omega_s'$  is the hour angle when the sun first strikes the inclined surface, calculated by Equation 13:

$$\omega_s' = \min \left[ \begin{array}{l} \cos^{-1}(-\tan\phi \tan\delta) \\ \cos^{-1}(-\tan(\phi - \beta) \tan\delta) \end{array} \right] \quad (13)$$

## 2.2. Calculation of Instantaneous Solar Radiation on an Inclined Surface

The instantaneous solar radiation incident on a horizontal surface outside the atmosphere  $I_o$  can be calculated using Equation 14:

$$I_o = \frac{12 \times 3600 G_{sc}}{\pi} \left[ 1 + 0.033 \cos\left(\frac{360d}{365}\right) \right] \cdot \left[ \cos\phi \cos\delta (\sin\omega_2 - \sin\omega_1) + \frac{2\pi(\omega_2 - \omega_1)}{360} \sin\phi \sin\delta \right] \quad (14)$$

Where  $\omega$  is the hour angle, which can be calculated based on solar time (ST) using Equation 15.  $\omega_2$  and  $\omega_1$  are the hour angles corresponding to the time interval in which the instantaneous value is calculated.

$$\omega = 15(ST - 12) \quad (15)$$

The ratio ( $r_d$ ) of the diffuse instantaneous radiation on a horizontal surface  $I_d$  to the total daily diffuse radiation  $H_d$  is equal to the ratio of instantaneous extraterrestrial solar radiation  $I_o$  to daily total extraterrestrial radiation  $H_o$ , as defined in Equation 16:

$$r_d = \frac{I_d}{H_d} = \frac{I_0}{H_0} \quad (16)$$

The instantaneous solar radiation on a horizontal surface can be calculated using the ratio  $r_t$  defined in Equation 17 and applied in Equation 18:

$$r_t = \frac{\pi}{4N} \left\{ \cos \left( \frac{180}{2} \frac{\omega}{\omega_s} \right) + \frac{2}{\sqrt{\pi}} (1 - \Psi) \right\} \quad (17)$$

$$r_t = \frac{I}{H} \quad (18)$$

Here,  $\omega$  represents the hour angle at the midpoint between two solar time (ST) intervals.

$\Psi$  is defined as below:

$$\Psi = \exp \left\{ -4 \left( 1 - \frac{|\omega|}{\omega_s} \right)^2 \right\} \quad (19)$$

The instantaneous solar radiation on a horizontal surface  $I$  consists of both diffuse  $I_d$  and direct  $I_b$  components:

$$I = I_d + I_b \quad (20)$$

Using the value of  $I$  obtained from Equation 18 and  $I_d$  from Equation 16,  $I_b$  can be calculated with Equation 20.

The instantaneous solar radiation incident on an inclined surface,  $I_T$ , comprises direct  $I_{bT}$ , diffuse  $I_{dT}$ , and reflected  $I_{refT}$  radiation components:

$$I_T = I_{bT} + I_{dT} + I_{refT} \quad (21)$$

The diffuse component of the instantaneous solar radiation on an inclined surface  $I_{dT}$  can be calculated using Equation 22:

$$I_{dT} = I_d \frac{1 + \cos \beta}{2} \quad (22)$$

The direct component of the instantaneous solar radiation on an inclined surface  $I_{bT}$  can be calculated using Equation 23:

$$I_{bT} = R_b \cdot I_b \quad (23)$$

Where  $R_b$  is the geometric factor, defined in Equation 24:

$$R_b = \frac{\cos \theta}{\cos \theta_z} \quad (24)$$

$\theta$  is the solar incidence angle, calculated with Equation 25:

$$\cos \theta = \sin \delta \sin \phi \cos \beta - \sin \delta \cos \phi \sin \beta \cos \gamma + \cos \delta \cos \phi \cos \beta \cos \omega + \cos \delta \sin \phi \sin \beta \cos \gamma \cos \omega + \cos \delta \sin \beta \sin \gamma \sin \omega \quad (25)$$

Here,  $\gamma$  is the surface azimuth angle, which is  $0^\circ$  for south-facing,  $180^\circ$  for north-facing,  $270^\circ$  for east-facing, and  $90^\circ$  for west-facing surfaces.

$\theta_z$  is the zenith angle, representing the solar incidence angle on a horizontal surface ( $\beta = 0$ ), as defined in Equation 26:

$$\cos\theta_z = \cos\delta\cos\phi\cos\beta\cos\omega + \sin\delta\sin\phi \quad (26)$$

Instantaneous reflected radiation  $I_{refT}$  on an inclined surface is defined in Equation 27:

$$I_{refT} = I\rho\left(\frac{1-\cos\beta}{2}\right) \quad (27)$$

### 2.3. Solution Procedure

This section presents the core methodology developed for this study, based on theoretical radiation models and numerical optimization techniques, to calculate and compare solar gains across four surface configurations.

Using the theoretical calculations for daily and instantaneous solar radiation defined in Sections 2.1 and 2.2, mathematical models were developed in MS Excel for four surface types: a horizontal surface, a fixed south-facing inclined surface, an east-west tracking surface, and a south-north tracking surface. The Konya province in Turkey, which has high solar energy potential and favorable economic and topographic conditions for solar power plant installations, was selected as the study area. The study area is located at  $37.97^\circ\text{N}$  latitude and  $32.57^\circ\text{E}$  longitude, with an altitude of 1031 meters above sea level.

The input parameters used in the mathematical model are summarized in Table 3.

**Table 3.** Input parameters for the mathematical model

Parameter Description	Symbol	Value / Source
The latitude angle ( $^\circ$ )	$\phi$	37.97
The altitude (m)	$Z$	1031
The average day value of month	$d$	(Table 1) [38]
Actual sunshine duration (h) of month	$n$	(Table 2) [39]
Tilt angle of the surface ( $^\circ$ )	$\beta$	Iteratively optimized via Solver add-in.
Reflection coefficient	$\rho$	0.7 (Dec, Jan, Feb), 0.2 (others) [40]
Solar time (h)	$ST$	Examined time
Surface azimuth angle ( $^\circ$ )	$\gamma$	$0^\circ$ for south-facing, $180^\circ$ for north-facing, $270^\circ$ for east-facing, and $90^\circ$ for west-facing surfaces
The solar constant ( $\text{W}/\text{m}^2$ )	$G_{sc}$	1367

The daily solar radiation on the horizontal surface was calculated using the average day of each month, and the resulting monthly values were summed to determine the annual total. Figure 1 illustrates the step-by-step procedure for calculating daily solar radiation on a horizontal surface.



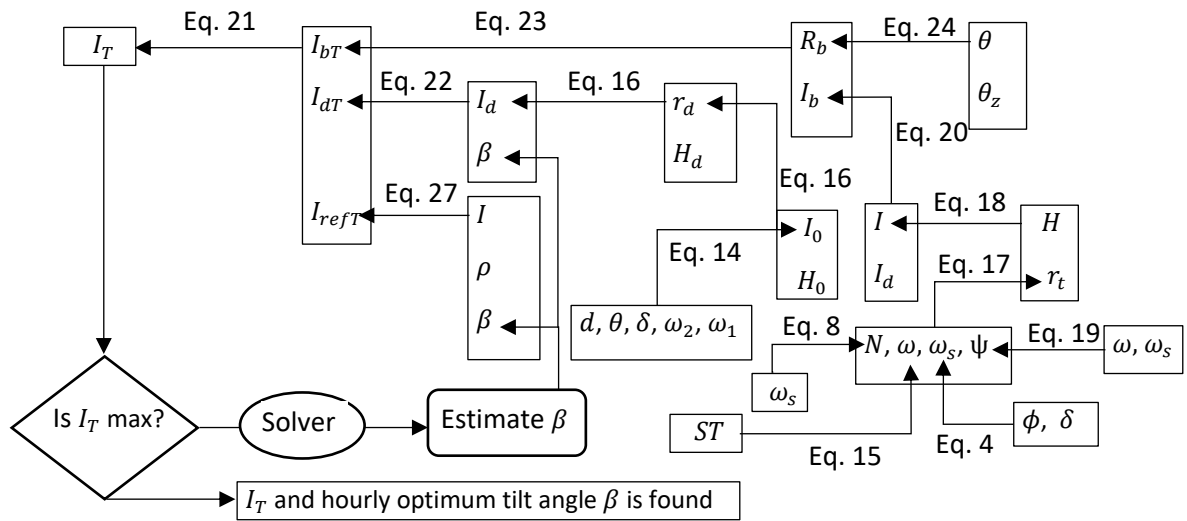


**Figure 3.** Procedure for determining optimal tilt angles for maximum instantaneous radiation in inclined tracking surface

### 3. RESULTS AND DISCUSSION

In this study, the solar radiation gains of four surface configurations were compared specifically for the Konya province in Turkey: an east-west tracking surface, a south-north tracking surface, a fixed south-facing inclined surface optimized for maximum annual solar radiation gain, and a horizontal surface. The Konya region, selected as the study area due to its geographical and economic suitability for solar power plant installations in Turkey, provides favorable conditions for solar energy generation.

#### 3.1. Monthly And Hourly Variation of Tilt Angles for Tracking Surfaces

On the representative (average) day of each month, the tilt angles that yield the maximum instantaneous solar radiation for each hour were determined for both east-west and south-north tracking surfaces. These calculations were conducted for the study region using the mathematical modeling and Solver-based optimization approach detailed in Section 2.3. The resulting hourly optimum tilt angles are summarized in Table 4 and Table 5, respectively.

**Table 4.** Calculated monthly and hourly tilt angles for the east-west solar tracking system in the selected region

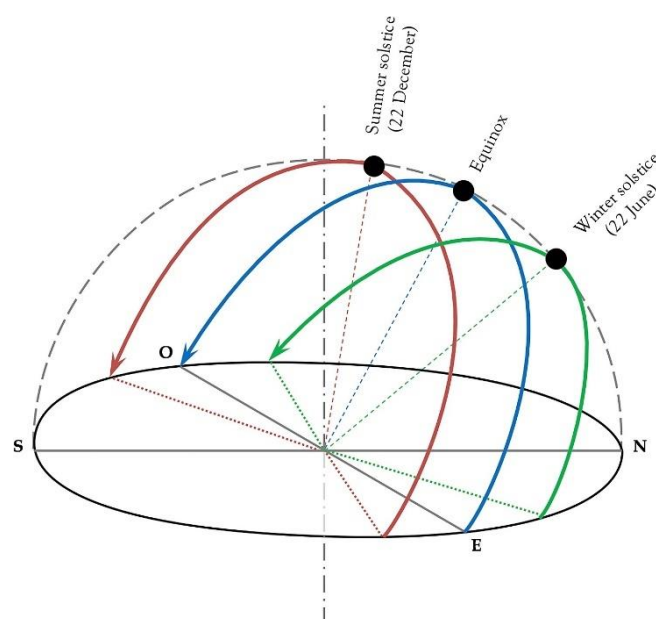
Solar Time	Jan	Feb	Mar	Apr	May	Jun	Jul	Aug	Sep	Oct	Nov	Dec
5:30					81,4°	78,9°	80,7°	86,6°				
6:30			81,4°	74,2°	69,0°	67,3°	69,0°	73,9°	80,6°			
7:30		80,4°	68,1°	62,0°	57,5°	56,2°	57,8°	62,1°	68,0°	73,7°	77,5°	
8:30	63,6°	70,8°	55,1°	49,5°	45,6°	44,6°	46,0°	49,9°	55,1°	60,4°	64,9°	75,2°
9:30	49,0°	58,2°	40,7°	36,1°	33,1°	32,4°	33,6°	36,6°	40,9°	45,4°	49,7°	63,5°
10:30	30,7°	40,2°	24,9°	21,9°	20,0°	19,6°	20,4°	22,4°	25,3°	28,3°	31,3°	45,4°
11:30	10,5°	14,8°	8,4°	7,3°	6,7°	6,6°	6,9°	7,6°	8,6°	9,6°	10,7°	17,3°
12:30	-10,5°	-14,8°	-8,4°	-7,3°	-6,7°	-6,6°	-6,9°	-7,6°	-8,6°	-9,6°	-10,7°	-17,3°
13:30	-30,7°	-40,2°	-24,9°	-21,9°	-20,0°	-19,6°	-20,4°	-22,4°	-25,3°	-28,3°	-31,3°	-45,4°
14:30	-49,0°	-58,2°	-40,7°	-36,1°	-33,1°	-32,4°	-33,6°	-36,6°	-40,9°	-45,4°	-49,7°	-63,5°
15:30	-63,6°	-70,8°	-55,1°	-49,5°	-45,6°	-44,6°	-46,0°	-49,9°	-55,1°	-60,4°	-64,9°	-75,2°
16:30		-80,4°	-68,1°	-62,0°	-57,5°	-56,2°	-57,8°	-62,1°	-68,0°	-73,7°	-77,5°	
17:30			-81,4°	-74,2°	-69,0°	-67,3°	-69,0°	-73,9°	-80,6°			
18:30					-81,4°	-78,9°	-80,7°	-86,6°				

**Table 5.** Calculated monthly and hourly tilt angles for the south-north solar tracking system in the selected region

Solar Time	Jan	Feb	Mar	Apr	May	Jun	Jul	Aug	Sep	Oct	Nov	Dec
5:30					-66,8°	-64,9°	-67,1°	-77,8°				
6:30			37,2°	-10,2°	-26,3°	-31,7°	-30,6°	-20,7°	16,9°			
7:30	70,2°	69,5°	35,9°	12,0°	-3,2°	-9,2°	-6,9°	5,5°	28,8°	53,8°	68,0°	
8:30	71,7°	63,6°	36,4°	19,8°	7,8°	2,7°	5,2°	15,5°	31,9°	48,4°	60,1°	73,6°
9:30	67,9°	60,6°	36,4°	23,1°	13,2°	9,0°	11,3°	20,1°	33,1°	46,0°	55,7°	69,8°
10:30	65,6°	58,9°	36,2°	24,7°	16,0°	12,2°	14,4°	22,3°	33,6°	44,6°	53,2°	67,3°
11:30	64,4°	58,1°	36,0°	25,3°	17,1°	13,6°	15,7°	23,2°	33,7°	44,0°	51,9°	66,1°
12:30	64,4°	58,1°	36,0°	25,3°	17,1°	13,6°	15,7°	23,2°	33,7°	44,0°	51,9°	66,1°
13:30	65,6°	58,9°	36,2°	24,7°	16,0°	12,2°	14,4°	22,3°	33,6°	44,6°	53,2°	67,3°
14:30	67,9°	60,6°	36,4°	23,1°	13,2°	9,0°	11,3°	20,1°	33,1°	46,0°	55,7°	69,8°
15:30	71,7°	63,6°	36,4°	19,8°	7,8°	2,7°	5,2°	15,5°	31,9°	48,4°	60,1°	73,6°
16:30	70,2°	69,5°	35,9°	12,0°	-3,2°	-9,2°	-6,9°	5,5°	28,8°	53,8°	68,0°	
17:30			37,2°	-10,2°	-26,3°	-31,7°	-30,6°	-20,7°	16,9°			
18:30					-66,8°	-64,9°	-67,1°	-77,8°				

The east-west tracking system follows the sun's path from sunrise to sunset along the same axis. As the summer solstice approaches and the days lengthen, the start and end times of solar tracking shift to earlier and later hours. At solar noon, 12:00, when the sun is at its highest position, a horizontal orientation provides the maximum radiation gain.

The south-north tracking system does not exhibit a similar directional pattern throughout the year as the east-west tracking system does. This difference is primarily due to the sun's varying path across the sky throughout the year, as illustrated in Figure 4. During the spring and autumn equinoxes, the sun rises and sets exactly in the east and west, respectively; in summer, it shifts northward, rising and setting in more northerly directions, while in winter, it remains in the southern hemisphere throughout the day. As the sun's rising and setting directions deviate from the east-west line, the start and end angles of the south-north tracking system become increasingly steep. In December, the starting and ending angle of the system faces south at 73.6°, whereas in June, due to the sun rising from the north, this angle shifts to -64.9°, pointing northward. In April and September, the surface starts the day at a near-horizontal angle of -10.2° and 16.9°, respectively.

**Figure 4.** The path of the sun in the sky throughout the year in the southern hemisphere [41]

### 3.2. Monthly and Annual Total Solar Radiation on Surfaces

Daily total radiation values were calculated for each surface configuration—east-west tracking, south-north tracking, fixed south-facing surface with optimal tilt angle, and horizontal surface—based on the average day of each month. From these calculations, monthly and annual total gain values were determined. The calculated annual total solar radiation values for each surface type are presented in Table 5. The lowest annual total solar radiation falls on the horizontal surface. The fixed south-facing surface with an optimal tilt angle of  $28.58^\circ$ , which provides the maximum annual gain, collects 9% more radiation than the horizontal surface. Meanwhile, the south-north tracking surface achieves a 16% higher radiation gain, and the east-west tracking surface provides a 30% higher gain than horizontal surface. Consequently, the east-west tracking system is identified as the most suitable single-axis tracking method for the Konya region in terms of annual total gain.

**Table 5.** Calculated annual total solar radiation on surfaces in in the selected region

Surface Type	East-West Tracking	South-North Tracking	Fixed Tilt	Horizontal
Annual Total Radiation	2074 kWh/m <sup>2</sup> /year	1845 kWh/m <sup>2</sup> /year	1738 kWh/m <sup>2</sup> /year	1597 kWh/m <sup>2</sup> /year
Gain compared to Horiz.	30%	16%	9%	-

The daily total solar radiation values for each surface, calculated using the mathematical model and Solver-based procedure described in Section 2.3, based on the average day of each month, are shown in Figure 5 for comparison. The advantage of the east-west tracking surface becomes especially evident in the summer months. For example, in June, the south-north tracking surface collects an average of 6.96 kWh/m<sup>2</sup> of radiation daily, while the east-west tracking surface receives 2.02 kWh/m<sup>2</sup> more, reaching 8.98 kWh/m<sup>2</sup>. In winter, however, the east-west tracking surface receives less solar radiation than the south-north tracking surface. This is due to the sun's southward path throughout winter, which prevents the east-west tracking surface from focusing on the south. In December, for example, the south-north tracking surface collects an average of 2.12 kWh/m<sup>2</sup> of radiation daily, while the east-west tracking surface receives 1.69 kWh/m<sup>2</sup>, resulting in a 0.43 kWh/m<sup>2</sup> lower gain.

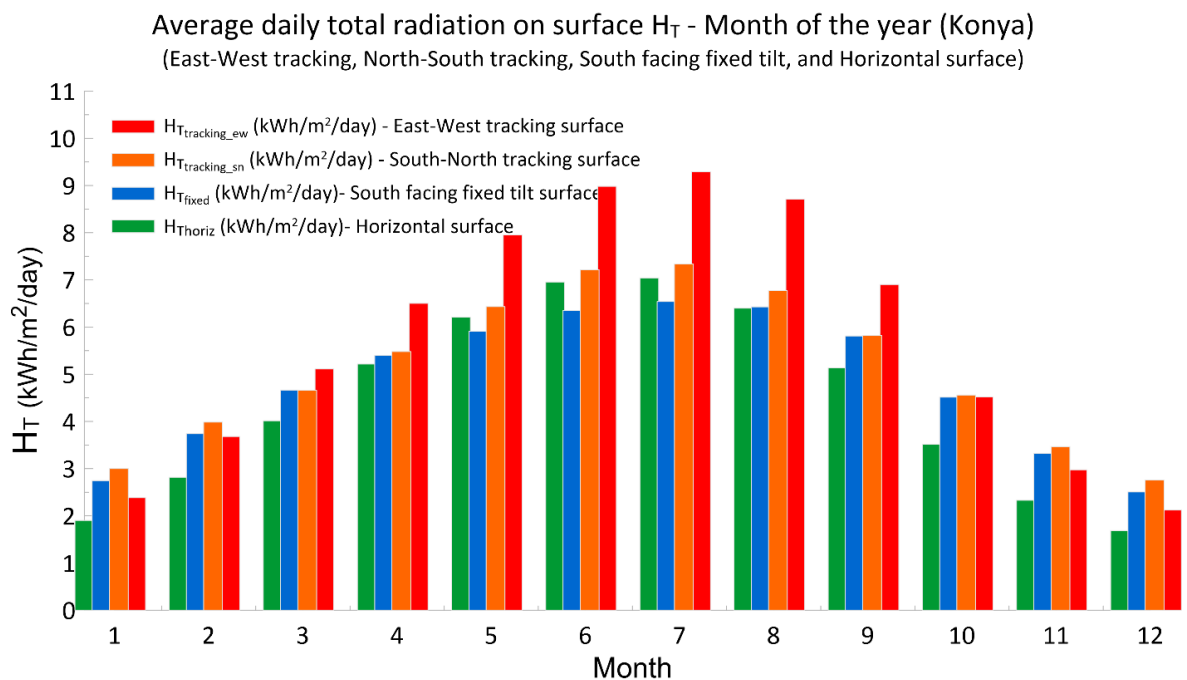


**Figure 5.** Monthly variation of daily total radiation on east-west tracking, south-north tracking, fixed-tilt, and horizontal surfaces in Konya

In conclusion, the east-west tracking system offers an advantage in terms of annual gain, while the south-north tracking system performs more effectively during the winter season. The fixed-tilt surface, compared to the horizontal surface, provides higher radiation gain throughout the year except in May, June, and July. The south-north tracking surface, always oriented at the optimal angle toward the south at any hour of the year, consistently collects more solar radiation than both the horizontal and fixed-tilt systems each month.

### 3.3. Hourly Variation of Instantaneous Solar Radiation on Surfaces in June and December

The values presented in this section were obtained using the solution procedure described in Section 2.2 and the calculation workflow shown in Figure 3, which determines both the instantaneous solar radiation and the corresponding optimal tilt angles for inclined tracking surfaces.

The calculated hourly variation of instantaneous solar radiation on east-west tracking, south-north tracking, fixed-tilt, and horizontal surfaces for the month of June is presented in Figure 6. As expected, the advantage of the east-west tracking surface becomes apparent in the morning and evening hours when the sun is positioned in the east and west. Around midday, when the sun is near its peak, both tracking systems approach a horizontal position and receive a similar amount of solar radiation. The fixed-tilt surface, set at the angle for optimal annual gain, collects lower radiation in June compared to the horizontal surface, particularly in the morning and evening. This is primarily due to the south-facing surface's reduced ability to capture sunlight from the sun's northward path, in contrast to the horizontal surface.

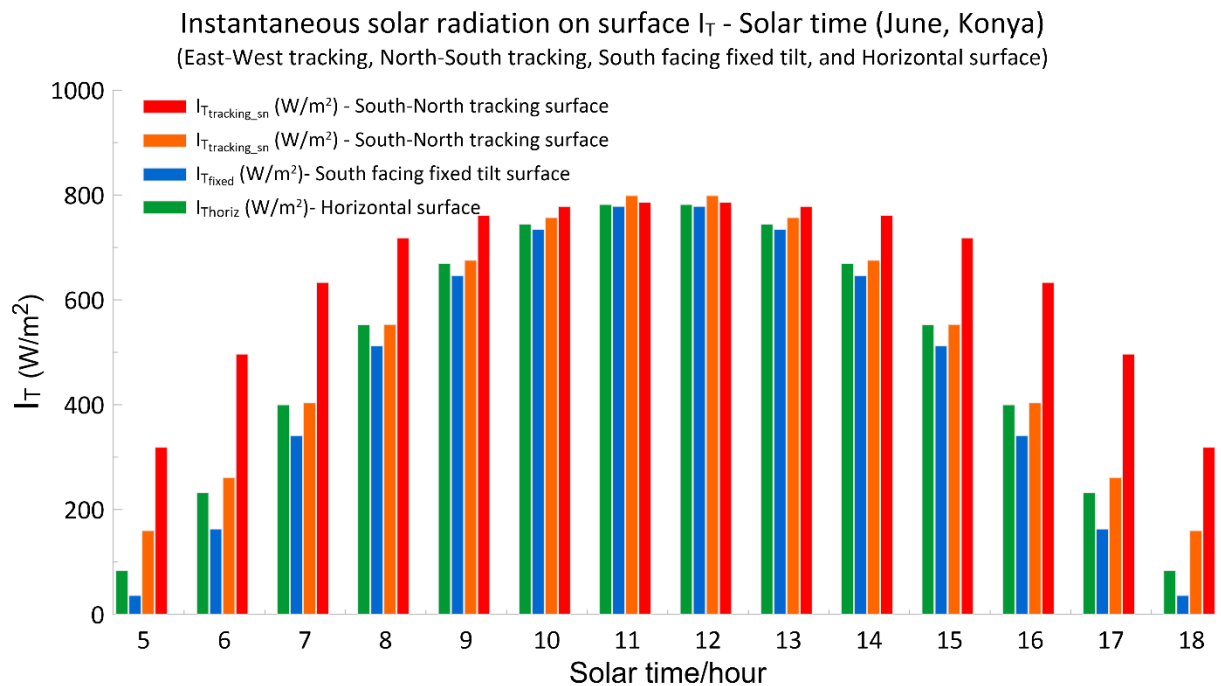


**Figure 6.** Hourly variation of instantaneous radiation on east-west tracking, south-north tracking, fixed-tilt, and horizontal surfaces in selected region during June

Figure 7 presents the hourly variation of instantaneous solar radiation on east-west tracking, south-north tracking, fixed-tilt, and horizontal surfaces for the month of December. In December, the sun is positioned significantly southward and reaches the earth from a tilted angle even at midday. The east-west tracking surface cannot fully utilize this southern sunlight and, therefore, collects less solar radiation during midday compared to south-facing surfaces. For instance, between 12:00 and 13:00, the instantaneous radiation on the south-north tracking surface is 462.2 W/m<sup>2</sup>, whereas the east-west tracking surface receives only 297.4 W/m<sup>2</sup>. The instantaneous radiation on the fixed-tilt surface,

however, reaches 402.9 W/m<sup>2</sup> during this time period, making it more advantageous than the east-west tracking system, which aligns closer to the horizontal at noon.

In the morning, as the sun rises from the east, the east-west tracking surface collects 176.2 W/m<sup>2</sup> of instantaneous radiation between 08:00 and 09:00. This value is only slightly higher than the 165.2 W/m<sup>2</sup> received by the south-north tracking surface, resulting in an insignificant gain in total radiation.

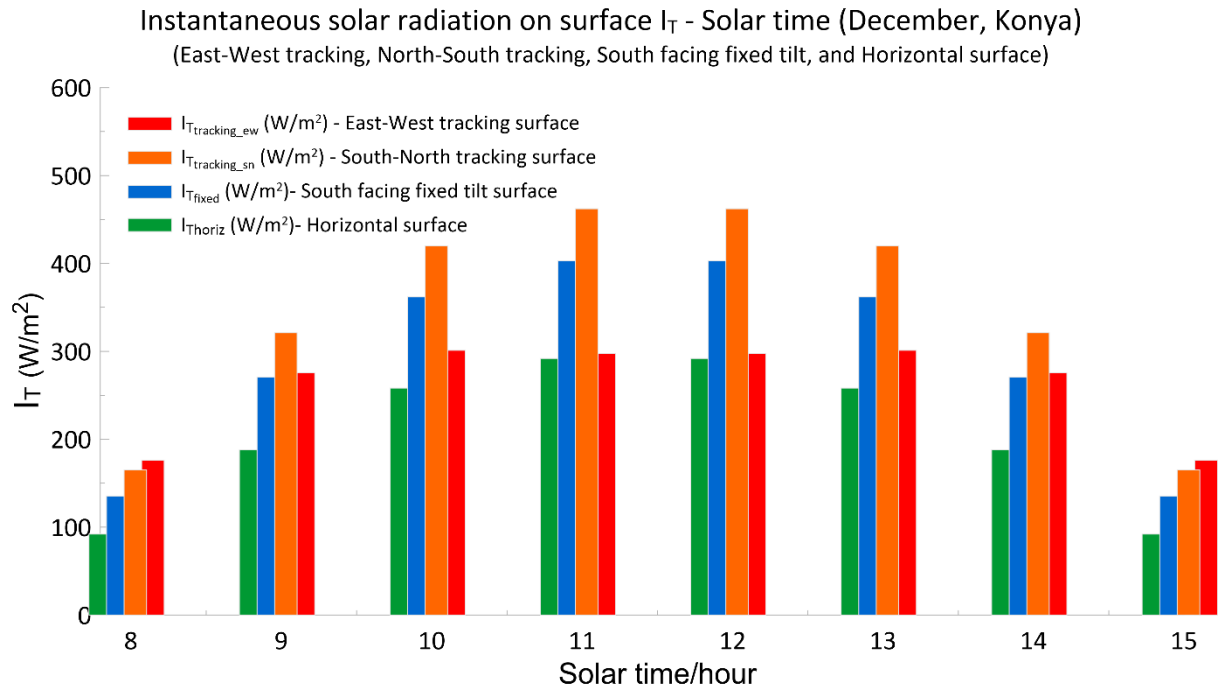


**Figure 7.** Hourly variation of instantaneous radiation on east-west tracking, south-north tracking, fixed-tilt, and horizontal surfaces in selected region during December

In conclusion, the east-west tracking surface provides an additional gain of up to 2 kWh/m<sup>2</sup> daily compared to the south-north tracking surface, particularly during the summer months. In winter, however, the south-north tracking system can offer a higher gain of up to 0.4 kWh/m<sup>2</sup> daily. Therefore, for applications prioritizing annual gains, such as PV electricity generation plants, the east-west tracking system would be a suitable choice. In applications focused on winter performance, the south-north tracking system presents a more advantageous option. This is especially true in conditions where environmental factors obstruct the sunrise and sunset, making the south-north tracking system even more favorable in winter. Future studies could further evaluate the annual, monthly, and instantaneous gains of dual-axis tracking systems and compare their performance with single-axis tracking systems.

#### 4. CONCLUSIONS

In this study, the annual and seasonal solar radiation gains of single-axis solar tracking systems in two different orientations were analyzed specifically for the Konya region. For four surfaces—east-west tracking, south-north tracking, a fixed tilt angle optimized for annual gain, and a horizontal surface—the monthly average daily radiation and the annual total radiation values were calculated. The hourly variations in instantaneous solar radiation were also determined and compared for December and June. The findings reveal that solar radiation gains vary significantly by season, depending on surface orientation.

The east-west tracking system delivered the highest annual performance, capturing approximately 30% more radiation than the horizontal surface and 19% more than the fixed-tilt surface. During June, it also outperformed the south-north setup by 2.02 kWh/m<sup>2</sup> per day, a 29% increase, making it particularly

effective for applications such as photovoltaic (PV) power plants that prioritize annual energy production.

In contrast, during December, the south-north tracking system collected 0.43 kWh/m<sup>2</sup> more daily radiation than the east-west orientation—a 25% seasonal advantage due to its alignment with the sun's lower southern path. This makes the south-north orientation more favorable for winter-dominant energy needs or in regions where seasonal demand peaks in colder months.

The fixed-tilt surface, set to an optimal annual angle, achieved a 9% gain over the horizontal surface on an annual basis. While it consistently outperformed the horizontal surface throughout the year, it did not match the higher gains achieved by the tracking systems. Notably, the south-north tracking system, with its ability to maintain an optimal southward orientation year-round, provided consistently higher solar radiation than both the fixed-tilt and horizontal surfaces.

The hourly tracking angle values obtained in this study can be directly applied to tracking systems designed for the Konya region. Additionally, the solution method used in this study can be adapted for other regions, allowing for the creation of region-specific hourly angle tables.

In summary, for applications prioritizing annual yield, such as PV plants, the east-west tracking system provides the most efficient single-axis solution. However, for applications where winter performance is essential, the south-north tracking system is more effective. Future studies could build on these findings by analyzing dual-axis tracking systems, providing a more comprehensive comparison of annual, monthly, and hourly gains relative to single-axis systems. This would enable a deeper understanding of the optimal tracking configurations for diverse energy needs and seasonal variations.

#### **Declaration of Ethical Standards**

The authors declare that they have carried out this completely original study by adhering to all ethical rules including authorship, citation and data reporting.

#### **Declaration of Competing Interest**

The authors declared that they have no conflict of interest.

#### **Funding / Acknowledgements**

The author(s) received no financial support for the research.

#### **Data Availability**

Data supporting the findings of this study can be obtained from the corresponding author with reasonable requests to assist in scientific studies.

#### **REFERENCES**

- [1] N. Çetinkaya, "IMPROVING OF RENEWABLE ENERGY SUPPORT POLICY AND A PERFORMANCE ANALYSIS OF A GRID-CONNECTED 1 MWP PV POWER PLANT IN KONYA," (in en), *Selçuk Üniversitesi Mühendislik, Bilim Ve Teknoloji Dergisi*, vol. 5, no. 3, pp. 251-261, September 2017, doi: 10.15317/Scitech.2017.86.
- [2] M. Karimzadeh Kolamroudi, M. Ilkan, F. Egelioglu, and B. Safaei, "Maximization of the output power of low concentrating photovoltaic systems by the application of reflecting mirrors," *Renewable Energy*, vol. 189, pp. 822-835, 2022/04/01/ 2022, doi: <https://doi.org/10.1016/j.renene.2022.03.031>.
- [3] M. K. Kolamroudi, M. Ilkan, F. Egelioglu, and B. Safaei, "Feature selection by ant colony optimization and experimental assessment analysis of PV panel by reflection of mirrors

- perpendicularly," *Renewable Energy*, vol. 218, p. 119238, 2023/12/01/ 2023, doi: <https://doi.org/10.1016/j.renene.2023.119238>.
- [4] M. Karimzadeh Kolamroudi, M. Ilkan, F. Egelioglu, and B. Safaei, "A comparative study of LCPV by mirror reflection against other systems: Recent techniques, implications, and performances," *Solar Energy*, vol. 250, pp. 70-90, 2023/01/15/ 2023, doi: <https://doi.org/10.1016/j.solener.2022.12.017>.
- [5] B. Utomo, J. Darkwa, D. Du, and M. Worall, "Solar photovoltaic cooling and power enhancement systems: A review," *Renewable and Sustainable Energy Reviews*, vol. 216, p. 115644, 2025/07/01/ 2025, doi: <https://doi.org/10.1016/j.rser.2025.115644>.
- [6] S. Gressler, F. Part, S. Scherhauser, G. Obersteiner, and M. Huber-Humer, "Advanced materials for emerging photovoltaic systems – Environmental hotspots in the production and end-of-life phase of organic, dye-sensitized, perovskite, and quantum dots solar cells," *Sustainable Materials and Technologies*, vol. 34, p. e00501, 2022/12/01/ 2022, doi: <https://doi.org/10.1016/j.susmat.2022.e00501>.
- [7] M. H. Aksoy and M. K. Çalık, "PERFORMANCE INVESTIGATION OF BIFACIAL PHOTOVOLTAIC PANELS AT DIFFERENT GROUND CONDITIONS," (in en), *Konya Journal of Engineering Sciences*, vol. 10, no. 3, pp. 704-718, September 2022, doi: 10.36306/konjes.1116729.
- [8] H. Park, A. Öztürk, H. Park, and M. U. Khan, "UTILIZATION OF ROBOTICS FOR SOLAR PANEL CLEANING AND MAINTENANCE," (in en), *Konya Journal of Engineering Sciences*, vol. 7, no. 4, pp. 768-775, December 2019, doi: 10.36306/konjes.654942.
- [9] A. Kabul, F. Yiğit, and A. Duran, "ESTIMATING THE SOLAR EXERGY POTENTIAL OF SURFACES WITH DIFFERENT TILT ANGLES," (in en), *Konya Journal of Engineering Sciences*, vol. 12, no. 3, pp. 756-772, September 2024, doi: 10.36306/konjes.1473068.
- [10] E. Akpınar, G. Gül Katircioglu, and M. Das, "Effects of solar tracking on different types of solar panels; experimental study for thermal and photovoltaic types," *International Journal of Hydrogen Energy*, 2025/02/17/ 2025, doi: <https://doi.org/10.1016/j.ijhydene.2025.02.155>.
- [11] B. Singh, P. Kaur, A. K. Yadav, M. K. Awasthi, and A. Kumar, "Design and Analysis of Solar Tracking System for PV Thermal Performance Enhancement," in *Heat Transfer Enhancement Techniques*, 2025, pp. 251-267.
- [12] M. Kabilan, V. Manikandan, and S. Dharshini, "Automatic Solar Tracking System: A Comprehensive Overview of an advanced Automatic Solar Tracking system using ESP8266," *Asian Journal of Applied Science and Technology (AJAST)*, vol. 9, no. 1, pp. 11-20, 2025.
- [13] K. Kumba, P. Upender, P. Buduma, M. Sarkar, S. P. Simon, and V. Gundu, "Solar tracking systems: Advancements, challenges, and future directions: A review," *Energy Reports*, vol. 12, pp. 3566-3583, 2024/12/01/ 2024, doi: <https://doi.org/10.1016/j.egy.2024.09.038>.
- [14] H. A. Kazem, M. T. Chaichan, A. H. A. Al-Waeli, and K. Sopian, "Recent advancements in solar photovoltaic tracking systems: An in-depth review of technologies, performance metrics, and future trends," *Solar Energy*, vol. 282, p. 112946, 2024/11/01/ 2024, doi: <https://doi.org/10.1016/j.solener.2024.112946>.
- [15] N. Kuttybay *et al.*, "Assessment of solar tracking systems: A comprehensive review," *Sustainable Energy Technologies and Assessments*, vol. 68, p. 103879, 2024/08/01/ 2024, doi: <https://doi.org/10.1016/j.seta.2024.103879>.
- [16] A. Bahrami, C. O. Okoye, and U. Atikol, "Technical and economic assessment of fixed, single and dual-axis tracking PV panels in low latitude countries," *Renewable Energy*, vol. 113, pp. 563-579, 2017/12/01/ 2017, doi: <https://doi.org/10.1016/j.renene.2017.05.095>.
- [17] K. Kumba, S. P. Simon, K. Sundareswaran, P. S. R. Nayak, K. A. Kumar, and N. P. Padhy, "Performance Evaluation of a Second-Order Lever Single Axis Solar Tracking System," *IEEE Journal of Photovoltaics*, vol. 12, no. 5, pp. 1219-1229, 2022, doi: 10.1109/JPHOTOV.2022.3187647.
- [18] A. Alshaabani, "Developing the Design of Single-Axis Sun Sensor Solar Tracking System," *Energies*, vol. 17, no. 14, doi: 10.3390/en17143442.
- [19] Z. Er and E. Balcı, "Dual axis solar angle tracking system without any sensor," (in en), *Journal of Energy Systems*, vol. 2, no. 3, pp. 127-136, September 2018, doi: 10.30521/jes.456606.

- [20] H. Toylan, "DESIGN AND APPLICATION OF SOLAR TRACKING SYSTEM USING OPTIMIZED FUZZY LOGIC CONTROLLER BY GENETIC ALGORITHM," (in en), *Mugla Journal of Science and Technology*, vol. 6, no. 1, pp. 136-145, June 2020, doi: 10.22531/muglajsci.641904.
- [21] A. Attou, A. Massoum, and M. Saidi, "Photovoltaic Power Control Using MPPT and Boost Converter," (in en), *Balkan Journal of Electrical and Computer Engineering*, vol. 2, no. 1, pp. 23-27, March 2014. [Online]. Available: <https://dergipark.org.tr/tr/pub/bajece/issue/3360/46444>  
<https://dergipark.org.tr/tr/download/article-file/39741>.
- [22] M. A. Khan and M. E. Tacer, "PV Panel Based Micro Inverter Using Boost Control Topology with PWM and MPPT (Perturb and Observe) Method," (in en), *International Journal of Electronics Mechanical and Mechatronics Engineering*, vol. 10, no. 1, pp. 1785-1794, January 2020. [Online]. Available: <https://dergipark.org.tr/tr/pub/ijemme/issue/65301/1005821>  
<https://dergipark.org.tr/tr/download/article-file/2013945>.
- [23] G. Nazlı Arpacı, P. D. M. C. Taplamacıoğlu, and D. D. H. Gözde, "Design and Comparison of Perturb & Observe and Fuzzy Logic Controller in Maximum Power Point Tracking System for PV System by Using MATLAB/Simulink," (in en), *International Journal of Multidisciplinary Studies and Innovative Technologies*, vol. 3, no. 1, pp. 66-71, March 2019. [Online]. Available: <https://dergipark.org.tr/tr/pub/ijmsit/issue/43647/569324>  
<https://dergipark.org.tr/tr/download/article-file/732206>.
- [24] M. E. Başoğlu, R. Ünsal, and G. Çağırılıoğlu, "Realization of a Dual Axis Solar Tracking System," (in en), *Bilecik Şeyh Edebali Üniversitesi Fen Bilimleri Dergisi*, vol. 9, no. 1, pp. 52-61, June 2022, doi: 10.35193/bseufbd.991613.
- [25] F. Alhaj Omar, G. Gökkuş, and A. A. Kulaksız, "ŞEBEKEDEN BAĞIMSIZ FV SİSTEMDE MAKSİMUM GÜÇ NOKTASI TAKİP ALGORİTMALARININ DEĞİŞKEN HAVA ŞARTLARI ALTINDA KARŞILAŞTIRMALI ANALİZİ," (in tr), *Konya Journal of Engineering Sciences*, vol. 7, no. 3, pp. 585-594, September 2019, doi: 10.36306/konjes.613871.
- [26] C. Sungur, "Multi-axes sun-tracking system with PLC control for photovoltaic panels in Turkey," *Renewable Energy*, vol. 34, no. 4, pp. 1119-1125, 2009/04/01/ 2009, doi: <https://doi.org/10.1016/j.renene.2008.06.020>.
- [27] N. A. Kelly and T. L. Gibson, "Improved photovoltaic energy output for cloudy conditions with a solar tracking system," *Solar Energy*, vol. 83, no. 11, pp. 2092-2102, 2009/11/01/ 2009, doi: <https://doi.org/10.1016/j.solener.2009.08.009>.
- [28] G. Quesada, L. Guillon, D. R. Rouse, M. Mehrtash, Y. Dutil, and P.-L. Paradis, "Tracking strategy for photovoltaic solar systems in high latitudes," *Energy Conversion and Management*, vol. 103, pp. 147-156, 2015/10/01/ 2015, doi: <https://doi.org/10.1016/j.enconman.2015.06.041>.
- [29] A. ÖZTÜRK, B. DOĞAN, and M. YEŞİLYURT, "Energy, exergy, sustainability, and economic analyses of a grid-connected solar power plant consisting of bifacial PV modules with solar tracking system on a single axis," *Science and Technology for Energy Transition (STET)*, vol. 78, 2023.
- [30] İ. Kayri, "Fotovoltaik Uygulamalar İçin Kararlı Tek Eksenli Bir Güneş Takip Sistemi Tasarımı ve Uygulaması," (in tr), *Yüzüncü Yıl Üniversitesi Fen Bilimleri Enstitüsü Dergisi*, vol. 28, no. 2, pp. 432-450, August 2023, doi: 10.53433/yyufbed.1256765.
- [31] N. Arslanoğlu and A. Yiğit, "Parabolik Oluk Güneş Toplayıcılarının Simülasyonu ve Anlık Isıl Performanslarının İncelenmesi," (in tr), *Mühendis ve Makina*, vol. 63, no. 709, pp. 709-725, December 2022, doi: 10.46399/muhendismakina.1121249.
- [32] O. R. Alomar, O. M. Ali, B. M. Ali, V. S. Qader, and O. M. Ali, "Energy, exergy, economical and environmental analysis of photovoltaic solar panel for fixed, single and dual axis tracking systems: An experimental and theoretical study," *Case Studies in Thermal Engineering*, vol. 51, p. 103635, 2023/11/01/ 2023, doi: <https://doi.org/10.1016/j.csite.2023.103635>.
- [33] M. S. Azam *et al.*, "Performance enhancement of solar PV system introducing semi-continuous tracking algorithm based solar tracker," *Energy*, vol. 289, p. 129989, 2024/02/15/ 2024, doi: <https://doi.org/10.1016/j.energy.2023.129989>.

- [34] A. Celen, M. Y. Kaba, A. Kurnu Seyhan, and P. Celen, "FARKLI EĐİM AILARINDA GÜNEŐ KOLLEKTÖRLERİNİN ENERĐİ VE EKSERĐİ ANALİZİ: ERZİNCAN İLİ ÖRNEĐİ," (in tr), *Konya Journal of Engineering Sciences*, vol. 10, no. 3, pp. 634-648, September 2022, doi: 10.36306/konjes.1096936.
- [35] E. DoĐan and Y. Karakılık, "TÜRKİYE'DE GÜNEŐ PANELLERİNDEN ENERĐİ ÜRETİMİ: KONYA İLİ ÜZERİNE BİR DEĐERLENDİRME," (in tr), *KaramanoĐlu Mehmetbey Üniversitesi Sosyal Ve Ekonomik AraŐtırmalar Dergisi*, vol. 26, no. 46, pp. 471-485, June 2024. [Online]. Available: <https://dergipark.org.tr/tr/pub/kmusekad/issue/85312/1428767>  
<https://dergipark.org.tr/tr/download/article-file/3695682>.
- [36] B. Y. H. Liu and R. C. Jordan, "The interrelationship and characteristic distribution of direct, diffuse and total solar radiation," *Solar Energy*, vol. 4, no. 3, pp. 1-19, 1960/07/01/ 1960, doi: [https://doi.org/10.1016/0038-092X\(60\)90062-1](https://doi.org/10.1016/0038-092X(60)90062-1).
- [37] B. Liu and R. Jordan, "Daily insolation on surfaces tilted towards equator," (in English), vol. 10, 1961-10-01 1961, doi: Journal Name: ASHRAE J.; (United States); Journal Volume: 10.
- [38] A. YiĐit and İ. Atmaca, *Güneő Enerjisi*. Alfa Aktüel Yayınları, 2010.
- [39] "Güneő Enerjisi Potansiyel Atlası." Enerji İŐleri Genel MüdürlüĐü. <https://gepa.enerji.gov.tr/MyCalculator/> (accessed 25.09.2024, 2024).
- [40] "Resmi İklim İstatistikleri." Meteoroloji Genel MüdürlüĐü <https://www.mgm.gov.tr/veridegerlendirme/il-ve-ilceler-istatistik.aspx> (accessed 20.09.2024, 2024).
- [41] B. Malet-Damour, S. Guichard, A. P. Jean, F. Miranville, and H. Boyer, "SHADECO: A low-cost shadow-ring for diffuse measures: State of the art, principles, design and application," *Renewable Energy*, vol. 117, pp. 71-84, 2018/03/01/ 2018, doi: <https://doi.org/10.1016/j.renene.2017.09.083>.